

Pulse shaping of octave spanning femtosecond laser pulses

Bingwei Xu, Yves Coello, Vadim V. Lozovoy, D. Ahmasi Harris, and Marcos Dantus

Michigan State University, Department of Chemistry, East Lansing, Michigan 48824
dantus@msu.edu

Abstract: Characterization and pulse shaping of octave spanning femtosecond lasers poses a significant challenge. We have constructed a grating-based pulse shaper for an ultra-broad-bandwidth (620-1020 nm) femtosecond laser, and used it to compensate the phase distortions of the laser, spatial-light modulator and optics within 0.1 rad accuracy across the entire bandwidth using Multiphoton Intrapulse Interference Phase Scan (MIIPS) without a precompressor. The compensated transform limited pulses generated a second harmonic spectrum with a $12,260\text{ cm}^{-1}$ spectral width. Binary phase modulation was introduced by this pulse shaping system to demonstrate high resolution control of the second harmonic generation spectrum.

© 2006 Optical Society of America

OCIS codes: (320.7110) Ultrafast nonlinear optics; (320.5540) Pulse shaping

References and links

1. A. Baltuska, and T. Kobayashi, "Adaptive shaping of two-cycle visible pulses using a flexible mirror," *Appl. Phys. B* **75**, 427-443 (2002).
2. M. Yamashita, K. Yamane, and R. Morita, "Quasi-automatic phase-control technique for chirp compensation of pulses with over-one-octave bandwidth - Generation of few- to mono-cycle optical pulses," *IEEE J. Sel. Top. Quantum Electron.* **12**, 213-222 (2006).
3. T. Binhammer, E. Rittweger, R. Ell, F. X. Kartner, and U. Morgner, "Prism-based pulse shaper for octave spanning spectra," *IEEE J. Quantum Electron.* **41**, 1552-1557 (2005).
4. V. V. Lozovoy, I. Pastirk, and M. Dantus, "Multiphoton intrapulse interference. IV. Ultrashort laser pulse spectral phase characterization and compensation," *Opt. Lett.* **29**, 775-777 (2004).
5. B. W. Xu, J. M. Gunn, J. M. Dela Cruz, V. V. Lozovoy, and M. Dantus, "Quantitative investigation of the multiphoton intrapulse interference phase scan method for simultaneous phase measurement and compensation of femtosecond laser pulses," *J. Opt. Soc. Am. B* **23**, 750-759 (2006).
6. L. Xu, N. Nakagawa, R. Morita, H. Shigekawa, and M. Yamashita, "Programmable chirp compensation for 6-fs pulse generation with a prism-pair-formed pulse shaper," *IEEE J. Quantum Electron.* **36**, 893-899 (2000).
7. A. M. Weiner, "Femtosecond pulse shaping using spatial light modulators," *Rev. Sci. Instrum.* **71**, 1929-1960 (2000).
8. P. Baum, S. Lochbrunner, and E. Riedle, "Tunable sub-10-fs ultraviolet pulses generated by achromatic frequency doubling," *Opt. Lett.* **29**, 1686-1688 (2004).
9. K. A. Walowicz, I. Pastirk, V. V. Lozovoy, and M. Dantus, "Multiphoton intrapulse interference. I. Control of multiphoton processes in condensed phases," *J. Phys. Chem. A* **106**, 9369-9373 (2002).
10. V. V. Lozovoy, I. Pastirk, K. A. Walowicz, and M. Dantus, "Multiphoton intrapulse interference. II. Control of two- and three-photon laser induced fluorescence with shaped pulses," *J. Chem. Phys.* **118**, 3187-3196 (2003).
11. V. V. Lozovoy, J. C. Shane, B. W. Xu, and M. Dantus, "Spectral phase optimization of femtosecond laser pulses for narrow-band, low-background nonlinear spectroscopy," *Opt. Express* **13**, 10882-10887 (2005).
12. V. V. Lozovoy, and M. Dantus, "Systematic control of nonlinear optical processes using optimally shaped femtosecond pulses," *Chem. Phys. Chem.* **6**, 1970-2000 (2005).

1. Introduction

The quest for ultra-broad-bandwidth femtosecond laser pulses has progressed at a very fast rate during the last five years. In 2002, Baltuska *et al.*[1] used a double-pass non-collinear optical parametric amplifier (NOPA) system to deliver sub-4 fs visible-near-infrared pulses. They also used second-harmonic-generation frequency-resolved optical gating (SHG-FROG) and a feedback loop as a means for adaptive pulse compression. In 2006, Yamashita *et al.*[2] generated 2.8 fs pulses, in a system in which a hollow fiber filled with 3-atm argon gas was used to generate a 500 nm bandwidth. They used modified spectral phase interferometry for direct electric field reconstruction (M-SPIDER) and a pulse shaper for pulse compression. The shortest pulses directly from a laser system itself were generated by Binhammer *et al.*[3] who achieved 4.3 fs pulses directly from an oscillator. They used a Ti:sapphire oscillator whose intracavity dispersion was controlled by a combination of double chirped mirror pairs and a CaF₂ prism sequence. This oscillator was capable of generating pulses spanning over 450 nm. They used spectral phase interferometry for direct electric field reconstruction (SPIDER), a prism-pair precompressor and a prism-based pulse shaper for pulse compression.

Here, we demonstrate automated pulse characterization and compression using a grating-based pulse shaper without prism precompression using MIIPS [4, 5]. The second harmonic generation (SHG) spectrum from the transform limited pulses was observed spanning approaching 200 nm, which to the best of our knowledge, is the broadest SHG spectrum generated from laser pulses directly from an oscillator with and an SHG crystal. We demonstrate accurate pulse shaping for control of two-photon processes achieved by specially designed binary phase functions.

2. Experiments

We used a Ti:Sapphire oscillator (Ventec Pulse 1, Nanolayers GmbH) whose ultra-broad-bandwidth spectrum can exceed 400 nm producing ca. 1.5 nanojoule pulses at 75 MHz, and is

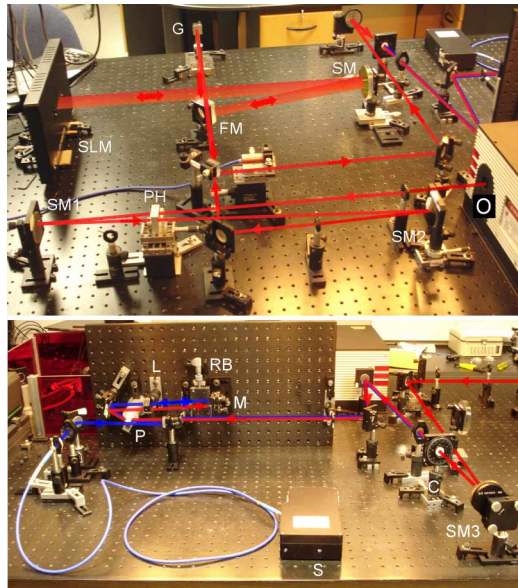


Fig 1. Experimental setup. O=oscillator, SM1 and SM2=reflective 1: 2.5 telescope, PH=pinhole, G=grating, FM=folding mirror, SM=spherical mirror, SLM=spatial light modulator, C = KDP crystal, SM3 =spherical mirror, P =prism, L =lens, RB=razor blade, M=mirror, S=spectrometer. Red and blue lines represent the fundamental and SHG beam, respectively.

very similar to that used by Binhammer and co-workers [3]. In their work, a prism-based pulse shaper such as the one used by Yamashita was used to shape the ultrashort pulses [6].

We found that the use of a prism-based pulse shaper introduces very large group velocity dispersion and third order dispersion that requires an additional prism-based pre-compressor. We calculated and confirmed experimentally that the prism in the pulse shaper introduced higher order phase distortions that could not be compensated by using a prism-pair compressor regardless of optical material. Therefore, our pulse shaper uses a single grating, eliminating the need for a prism pre-compressor.

The experimental setup used is shown in Fig. 1. The laser pulses from the oscillator (O) were first directed to a pair of spherical mirrors (SM1 and SM2) in order to expand the beam radius to 4 mm and collimate the beam. A 150- μm pinhole (PH) was placed at the focal point of the first spherical mirror to reduce the fluorescence from the oscillator, and to ensure better collimation. The laser was then directed into a pulse shaper consisting of an enhanced-aluminum coated 150 line-per-mm grating (G), a folding mirror (FM), a 762-mm-focal-length gold coated spherical (SM) mirror and a 640-pixel double-mask SLM (CRI, SLM-640) in a folded geometry [7] chosen to double the retardance that can be introduced by the SLM. The optical resolution on the SLM depends on the diameter of the beam and the focal length of the spherical mirror and in our case is approximately one SLM pixel width (100 μm). The SLM was calibrated pixel by pixel with 0.05 rad accuracy due to the large bandwidth of our laser. After the pulse shaper, the laser was focused onto a 20- μm type-I KDP crystal (C) by a 200-mm-focal-length spherical mirror (SM3). The SHG signal along with the fundamental laser pulses were collimated by a thin quartz lens and directed to the detection apparatus. The beam was first dispersed by a quartz prism (P) to separate the SHG light from the fundamental frequencies. All the frequency components were then focused by a quartz lens (L) with focal length 15 cm. A razor blade (RB) located at the Fourier plane was used to block the fundamental frequency components without loss of SHG light. The second harmonic frequencies were then retro-reflected (M) and directed into a spectrometer (O) (QE65000, Ocean Optics Inc.). Since the SHG signal was S-polarized, the detection apparatus was placed on a plate vertical to the optical table (see lower panel of Fig 1) to avoid the use of polarization rotators that could not adequately manage the large spectral bandwidth.

3. Results and discussion

We used MIIPS to characterize and compensate the phase distortion of the laser system. For the MIIPS scan, a reference function of the form $\alpha \sin(\gamma\omega + \delta)$ was used with $\alpha = \pi$, $\gamma = 7$ fs and δ is a parameter scanned from -0.5π to 3.5π . The SHG spectra were then recorded and generated the MIIPS traces as shown in Fig. 2. [4, 5]. The complexity of the phase distortions across the bandwidth of this laser required 10 MIIPS iterations.

Figure 3(a) illustrates the spectrum of the fundamental pulses (in log scale) and the residual phase after compensation of the phase distortion. With such a residual phase, the calculated pulse duration would be 4.6 fs. The longer wavelength edge of the spectrum looks noisier than the shorter wavelength because the spectrometer has lower spectral response and is thus less sensitive at longer wavelengths.

The fundamental and corresponding SHG spectrum obtained for transform limited pulses are also shown in Fig 3. Note that the SHG spectrum starts at 310 nm and ends at 500 nm, spanning over 12,260 cm^{-1} . (The spectrum span was measured from where the signals cannot be discriminated from noises, and the $\text{FW1}/e^2\text{M}$ of the spectrum is $\sim 118\text{nm}$.) This is the broadest SHG signal generated directly from an oscillator using the conventional normal incidence on the KDP crystal. Other schemes for broad bandwidth SHG include the work by Baum *et al.* [8]. They used a NOPA system to generate visible pulses and used a confocal frequency doubling scheme to generate a UV spectrum spanning $\sim 10,720 \text{cm}^{-1}$. In our setup the beam was directly focused on the KDP crystal.

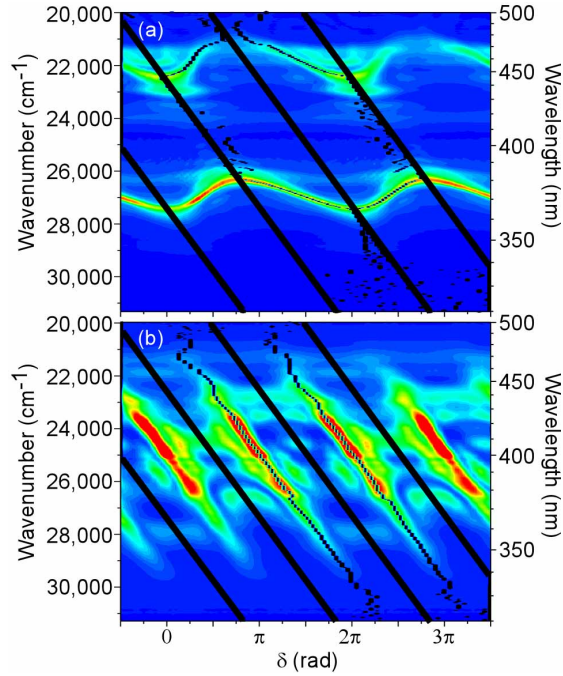


Fig. 2. MIIPS traces of the first (a) and last (b) iterations. Each vertical line of the MIIPS trace corresponds to a SHG spectrum generated at given value of δ (redder colors represent higher intensities). The black lines that separate the MIIPS traces are used to define the region for searching the maximum value of the SHG for each δ . The black dots within those boundaries show these maxima. The position of these maxima allows MIIPS to extract the phase. For TL pulses, the features form parallel lines separated by π .

The experimental result and the corresponding simulation using Fourier Transform without adjustable parameters and broadband corrections are shown below.

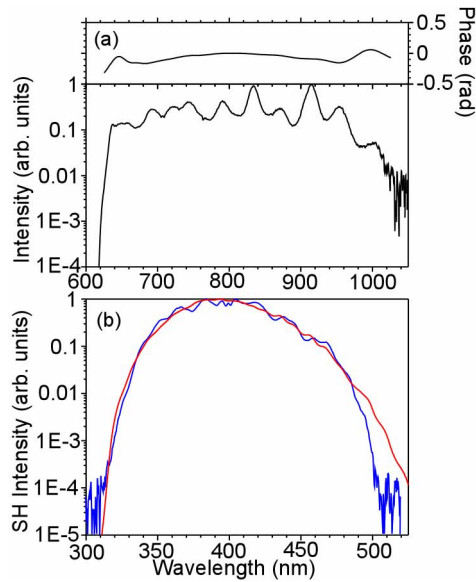


Fig. 3. (a) Spectrum of the fundamental pulses and residual phase after MIIPS compensation. (b) Measured (blue) and simulated (red) SHG spectra of the compensated pulses

The uncompressed output spectrum and the MIIPS retrieved spectral phase are shown in Fig. 4(a). In order to check the accuracy of the measurement, we used the retrieved phase and the measured spectrum to calculate the expected SHG spectrum. Figure 4(b) shows good agreement between the calculated spectrum and the experimentally measured SHG spectrum of the pulses prior to pulse compression. Some small features in the calculated spectrum are not present in our experimental data probably because of the low (~ 2.5 nm) spectrometer resolution. Since it is well-known that the SHG spectrum depends on the spectral phase of the laser pulses [9, 10], the good match between experimental data and theoretical prediction demonstrates that the retrieved phase from MIIPS was accurate (The statistical phase error or weighted average standard deviation for MIIPS has been measured to be as low as 0.01 rad across the bandwidth of the pulses[5]). As we can see from Fig. 4, the sharp peak in the SHG spectrum corresponds to the place in the fundamental spectrum where a point of inflection of the phase occurs.

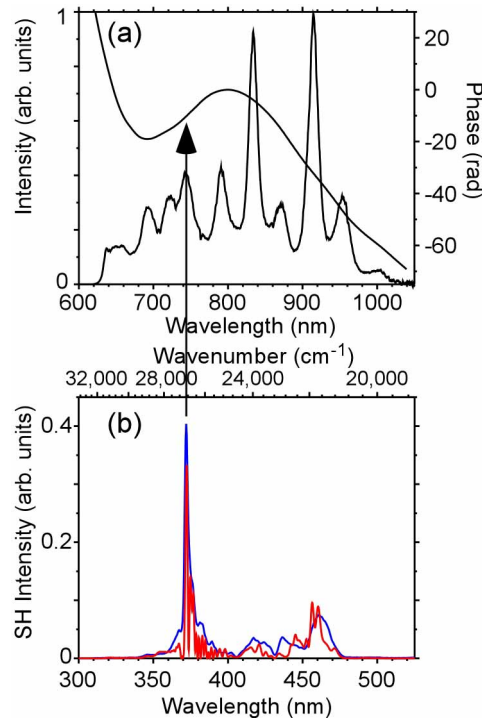


Fig. 4. (a) Spectrum of the fundamental pulses and residual phase after MIIPS compensation. (b) Measured (blue) and simulated (red) second harmonic spectra of the compensated pulses. The SHG spectrum was normalized with respect to the TL SHG spectrum intensity.

Figure 5 demonstrates our ability to accurately deliver ultra-broad-bandwidth shaped laser pulses. In these experiments, we chose several pseudorandom binary sequences [11] and generated binary sequences with points of symmetry and anti-symmetry in the frequency domain. Such binary phases generate sharp peaks at the point of symmetry and give very low background elsewhere, as was shown theoretically [12] and experimentally for pulses with less bandwidth [11]. Figure 5 shows an example in which a 120-bit binary phase containing 3 symmetrical sections was used. The left section is symmetric to the center section and the right section is anti-symmetric to the center section. One can clearly see that two peaks were generated in the SHG spectrum at the positions exactly corresponding to the symmetry points of the binary phase. The left peak corresponds to the point of symmetry of phase function, and can be used as criteria to confirm the precision of the phase modulation [12]. Note that the two peaks generated by the binary phase function are not related to the peaks in the SHG

